Friction and wear of PTFE composites with different filler in high purity hydrogen gas

Sawae, Yoshinori
Department of Mechanical Engineering, Faculty of Engineering, Kyushu University

Morita, Takehiro
Department of Mechanical Engineering, Faculty of Engineering, Kyushu University

Takeda, Kyota
STARLITE Co., Ltd.

Onitsuka, Shugo
Advanced Energy Materials Thrust, International Institute of Carbon-Neutral Energy Research, Kyushu University

他

出版情報：Tribology International. 157, pp.106884-, 2021-05. Elsevier
バージョン：
権利関係：

Friction and wear of PTFE composites with different filler in high purity hydrogen gas

Yoshinori Sawae [*1,2], Takehiro Morita [1,2], Kyota Takeda [3], Shugo Onitsu[2], Jyo Kaneuchi [3], Tetsuo Yamaguchi [1,2] and Joich Sugimura [1,2,4]

[1] Department of Mechanical Engineering, Faculty of Engineering, Kyushu University, Japan

[2] Advanced Energy Materials Thrust, International Institute of Carbon-Neutral Energy Research, Kyushu University, Japan

[3] STARLITE Co., Ltd., Japan

[4] Department of Tribology, Research Center for Hydrogen Industrial Use and Storage, Kyushu University, Japan

* sawae.yoshinori.134@m.kyushu-u.ac.jp

Abstract

Single-filler polytetrafluoroethylene (PTFE) composites with different filler materials are prepared and their tribological characteristics are evaluated in gaseous hydrogen to investigate the tribological function of each filler material. The results indicated that glass fibre caused severe abrasion on the cast iron sliding counterface and hence increased wear in both the composite and counterface in hydrogen. The friction and wear characteristics of polyphenylene sulphide-filled PTFE in hydrogen are similar to those in ambient air because it formed a PTFE-based transfer film on the counterface regardless of the surrounding atmosphere. On the other hand, carbon fibre-filled PTFE indicates excellent low friction and low wear in hydrogen. In this case, both the composite surface and sliding counterface are covered with carbon-rich tribofilms.

Keywords: PTFE; composite; hydrogen; piston ring

1. Introduction

Hydrogen is expected to be a clean and renewable energy carrier of the future [1][2][3]. It can be generated from many types of energy resources. In addition, it is suitable for mass transport and mass storage. A fuel cell vehicle (FCV) is a conspicuous example of the machine system utilising hydrogen. It is a type of electric vehicle that uses a fuel cell as its power source. FCVs use hydrogen gas instead of gasoline as their fuel and release only vapour during operation. Consequently, it is known as ‘ultimate ecologically friendly car’ and is expected to

contribute to the reduction in fossil fuel consumption and greenhouse gas emissions in the transportation sector. In addition, FCVs have distinctive practical advantages over battery electric vehicles, namely an elongated cruising distance and fast refuelling. The current generation of FCVs has a long cruising distance for the intercity transportation and can be refuelled within 5 min. Therefore, users of FCVs can enjoy usability similar to that of conventional gasoline cars [4][5].

Because the volumetric energy density of gaseous hydrogen is small, compressed hydrogen gas is used in FCVs to contain a sufficient amount of fuel on-board. The gas pressure should be increased using a mechanical gas compressor in refuelling stations such that it is sufficiently high to refuel the vehicle. The latest FCVs contain 70 MPa of hydrogen gas [3][6][7]. In this case, the hydrogen gas compressor is required to increase the gas pressure to approximately 100 MPa to fill the high-pressure storage tanks of the refuelling station at a gas pressure exceeding 80 MPa [7][8]. In addition, the fuel cell is susceptible to hydrogen gas contaminants. The allowable amount of each contaminant is regulated exactly by the ISO standard [9]. Consequently, the use of volatile lubricating oils and greases is strictly forbidden to maintain the purity of compressed hydrogen gas in mechanical compressors. To satisfy the abovementioned conditions, oil-free reciprocating compressors have been widely used in hydrogen refuelling stations. Key elements of the oil-free reciprocating compressor are gas-sealing elements, such as piston rings and rod packings [10][11][12]. These rings complete the seal between the piston and cylinder or around the piston rod for preventing gas leakage and ensuring gas compression. Since the sealing rings slide against the metal cylinder or the metal piston rod during the operation, they should function as tribological elements simultaneously and must satisfy the tribological requirements, such as low friction, low wear, and sealing performance [13][14]. The mechanical and tribological characteristics of these rings significantly affect the efficiency and reliability of compressors. If the piston rings exhibit excessive wear and unexpected fractures, it will increase the maintenance cost of compressors significantly and severely deteriorate the utilisation of the refuelling station.

Polytetrafluoroethylene (PTFE) has been widely used as a tribomaterial in various machine systems owing to its excellent self-lubrication ability and remarkable thermal and chemical stabilities [15][16]. However, PTFE has limited mechanical strength and wear resistance; therefore, it is typically used as a PTFE composite strengthened with several types of filler materials in tribological applications [15][17][18]. The friction and wear of PTFE composites with various filler materials have been studied extensively, and a large amount of knowledge has been collected. However, even now we find new publications for tribological study on PTFE composites in major scientific journals [19][20][21][22][23] because the range of tribological application of PTFE composites is steadily

increasing, and there is demand for improving it in some applications, including the piston ring for hydrogen gas compressors.

PTFE composites are widely used as piston ring materials for oil-free reciprocating gas compressors [10][11][12] not only because they can self-lubricate but also because compliant PTFE composite can easily conform to the sliding counterface, and a good sealing condition is readily obtained. For the compressor of hydrogen refuelling stations, the tribological requirements on the piston ring are quite severe. It should be sufficiently tough to withstand the extremely high gas pressure; exhibit high thermal stability to be used at approximately 150 ℃, to which the temperature of compressed hydrogen gas increases by adiabatic compression; and exhibit high wear resistance to maintain a reasonable lifetime under severe sliding conditions with a high sliding speed that exceeds 2 m/s at the most [7]. In addition, it slides against the metal counterface in a high-pressure and high-purity hydrogen gas environment.

Hydrogen is not inert in tribo-interfaces and imposes a unique effect on the friction and wear of tribological elements. The adverse effect of hydrogen on the mechanical strength of steels is well known as hydrogen embrittlement and significantly reduces the lifetime of rolling bearings [24][25][26]. By contrast, many studies have suggested the important role of hydrogen in the low-friction and wear characteristics of diamond-like carbon [27][28][29][30][31] and graphene [32][33]. Furthermore, certain effects of hydrogen on tribological behaviour have been reported for pure metals [34][35], steels [36], and polymers [37].

The tribological characteristics of polymer composites in hydrogen have been investigated experimentally in previous studies. Nosaka et al. investigated the friction and wear characteristics of PTFE composites in liquid hydrogen to identify the ideal material for a bearing retainer used in liquid hydrogen pumps for rocket engines [38][39]. Theiler et al. evaluated the friction and wear of various polymer composites with different resin and filler combinations in liquid hydrogen [40][41] and gaseous hydrogen [42][43][44][45].

The authors investigated the friction and wear of PTFE and PTFE composites in gaseous hydrogen under normal pressure [37][46] and high pressure [47][48] to understand the intrinsic effect of hydrogen. The main motivation of our polymer tribology studies in hydrogen is to improve the durability and reliability of piston rings used in the oil-free reciprocating hydrogen gas compressor for refuelling FCVs from the tribological aspect. However, available information regarding the mechanism associated with the tribological behaviour of PTFE composites in a hydrogen environment is limited and insufficient for establishing a knowledge base for the logical

material selection of piston rings. In particular, an appropriate understanding of the role of each filler material in polymer composites and their efficacy in the hydrogen gas environment is necessary to determine the ideal material composition of the piston ring and other tribological elements for hydrogen gas compressors and other machine elements in the hydrogen gas infrastructure.

The purpose of this study is to elucidate the tribological function of filler materials used in PTFE composites for hydrogen applications. We focused on four representative filler materials used in the PTFE composites for tribological applications. Single-filler PTFE composites with each filler material were prepared and sliding tests were conducted in high-purity hydrogen gas to evaluate their friction and wear behaviour. Both the composite surface and metal sliding counterface were analysed after performing the sliding test to better understand tribological phenomena at the sliding interface and to predict the effect of hydrogen on them. In particular, we focused on the formation of tribofilms on sliding surfaces as it has been reported to significantly affect the friction and wear processes of polymer materials [11][17][18][49][50][51][52].

2. Material and methods

2.1 Materials

Four filler materials were selected as research objectives in this study based on the composition of a referenced piston ring material used in current oil-free reciprocating hydrogen gas compressors. The ring material referenced in this study contains carbon fibre (CF) and polyphenylene sulphide (PPS) to reinforce the mechanical integrity of the composite. Therefore, CF and PPS were chosen as representative fillers for present piston rings. Two types of CF, Pitch-based CF (pitch-CF) and PAN-based CF (PAN-CF), were selected for the experiment because these CFs have clearly different dimensions and mechanical properties. Also, glass fibre (GF) was selected as another popular reinforcing filler for PTFE composites [53] to compare the results with CFs and PPS. Four single-filler composites were prepared using the same PTFE resin matrix with 20 wt% of each filler material. Cross-section images of the prepared PTFE composites are shown in Fig.1. The diameter of PAN-CF was smaller than that of pitch-CF and GF. Each fibre was incorporated into the composite as a short fibre filler, whereas PPS was used as a hard particle filler. All PTFE composites were prepared by STARLITE Co., Ltd. based on the same preparation procedure as commercially available PTFE composites for tribological applications. The bar stock of the arranged PTFE composites was machined into pin-shaped specimens with 15 mm length and 6 mm diameter. The pin surface was finished by turning and covered with residual machine marks. The pin specimen of pure PTFE

without filler materials was prepared and used as a control. The unfilled PTFE used in this study was made from same PTFE resin as the single-filler composites.

Grey cast iron (FC250) and tungsten carbide (WC) were used as materials for the sliding counterface. FC250 is a popular material for the cylinder block of oil-free reciprocating gas compressor whereas WC was used as a reference material with high surface hardness to exclude the contribution of counterface damage. Disk-shaped specimens with an outer diameter of 56 mm and a thickness of 3 mm were fabricated using both materials. The surface of the FC250 disk was finished by lapping with abrasive papers and the resultant disk surface had a surface roughness of Ra = 0.14 μm. Furthermore, the WC disks were finished with lapping; however, the surface roughness decreased when Ra = 0.04 μm. Vickers hardness of the FC250 disk and the WC disk were 241 and 1084, respectively.

All pin and disk specimens were cleaned ultrasonically for 10 min in a mixture of acetone and hexane. The cleaned specimens were subsequently weighed to determine their initial weights and stored in a dry cabinet until the sliding test.

2.2 Sliding test

For the prepared single-filler composites, their friction and wear behaviours in high purity hydrogen gas were analysed using a custom-made tribometre installed in a high-vacuum chamber equipped with a scroll vacuum pump and a turbo molecular vacuum pump. The chamber comprised a specially designed moisture controller developed by Fukuda [35] in front of its gas inlet to regulate the water content of hydrogen gas supplied to the chamber and maintain a constant level of gas purity for all sliding tests. The exhaust line from the chamber was connected to a cavity ring-down spectroscopy moisture sensor [54] and a Coulometric oxygen metre to confirm the purity of the hydrogen gas environment. Before starting the sliding test, the hydrogen gas was introduced to the moisture sensor and the oxygen metre from the chamber through the exhaust line. This was to evaluate the water and oxygen contents of the hydrogen gas environment. The obtained water content was less than 1 ppm (average 0.47 ppm), while the oxygen content was approximately 0.05 ppm. The water content was also measured after the sliding test. The water content increased and varied from 3 to 8 ppm after finishing the sliding test, probably because the water molecules adsorbed on the chamber wall were released into the hydrogen gas during the sliding test.

A schematic of the tribometre and specimen layouts in the chamber is shown in Fig. 2. The tribometre used in this study had a simple pin-on-disk configuration. The polymer pin specimen was clamped by the pin holder and loaded against the metal disk specimen by dead weights through a loading lever arm, whereas the disk specimen was rotated at a constant speed by a PC-controlled AC servo motor. The vertical contact force and tangentially exerted friction force at the sliding interface were measured by a biaxial load cell located between the pin holder and the lever arm. The outputs of the load cell were continuously monitored and accumulated in a datalogger as digital data. The data were subsequently analysed using a PC to describe the transition of the friction coefficient between the pin and disk specimens during the sliding test. After the sliding test, the pin and disk specimens were cleaned ultrasonically with a mixture of acetone and hexane and weighed using an electric balance to an accuracy of 0.01 mg. The volumetric wear rate of the polymer pin specimens and the gravimetric wear amount of the disk specimens were calculated from their weight change.

After setting the specimen for the tribometre, the chamber was sealed and evacuated to 10^{-4} Pa by vacuum pumps to reduce the effects of contaminants from residual air. Subsequently, hydrogen gas was supplied to the chamber through the moisture controller until the inner pressure of the chamber reached slightly less than the atmospheric pressure. The chamber was subsequently heated by an electric heater to increase the gas temperature and maintained for a time period such that the gaseous environment for the sliding test was the equilibrium condition at 373 K.

All sliding tests were performed under dry conditions with an average contact pressure of 1 MPa and a sliding speed of 2 m/s. After the initial 10000 m sliding, the pin and disk specimens were removed from the tribometre and cleaned based on the previously explained procedure to evaluate their weights. After rearranging the tribometre and the test environment with the same pin and disk specimens as described previously, the sliding test was continued for another 40000 m to evaluate the friction and wear characteristics of the PTFE composites. The data from the initial 10000 m sliding were not used for the evaluation to eliminate the contribution of initial high wear and unstable friction during the running in period.

The sliding test for the PTFE composites was conducted in atmospheric air under the same conditions without the surrounding atmosphere for comparison. In this case, the chamber was filled with ambient air after the tribometre was set up and heated to 373 K before starting the sliding test.

2.3 Surface analysis

After the sliding test, the worn surface of the composite pin specimen and the sliding track formed on the disk specimen were observed via optical microscopy. Subsequently, a laser Raman microscope (DXR2xi, Thermo Fisher Scientific) was used to obtain chemical information from the worn surface of the PTFE composites. Raman spectra were obtained from several points on the composite surface using 20X and 100X objectives with a 25 μm aperture. The wavelength and power of the excitation laser were 532 nm and 0.5 mW, respectively.

The chemical composition inside the sliding track on the disk surface was analysed using X-ray photoelectron spectrometry (XPS, JPS-9200KM, JEOL) with a monochromatic Al Kα X-ray source. The analysed spot size was 3 mm. To obtain the depth profile of the chemical compositions, XPS spectra were obtained iteratively after argon ion sputtering for 20, 60, 100, and 340 s. The accelerating voltage and the ion current of the sputtering in this study were 3 keV and 22.0 mA, respectively.

Further chemical analyses were conducted on the disk surface to characterise the transfer film formation from the PTFE composites. A chemical mapping function of an FT-IR microscope (Nicolet iN10MX, Thermo Fisher Scientific) and a laser Raman microscope (DXR2xi, Thermo Fisher Scientific) was employed to visualise the distribution of adhered PTFE and carbon in the sliding track formed on the disk surface. The IR measurement was conducted in the attenuated total reflection mode with a germanium prism and a 150 μm square aperture. IR spectra were obtained from 20 × 5 grid points within an 8 mm × 2 mm rectangular area around the sliding track. The typical IR spectrum contained characteristic peaks of C–F bonds in PTFE molecules and its fragments in the region from 1120 to 1280 cm^{-1}. Therefore, the area intensity of the IR peaks in this region was calculated for the obtained IR spectra and used as an index of the relative amount of adhered PTFE at each measuring point. Furthermore, Raman spectra were obtained from an 8 mm × 2 mm rectangular area; however, the number of measuring points was increased to 400 (40 ×10) because the pin hole size in the Raman microscope was much smaller than the aperture size in the FT-IR measurement; a 10X objective lens and a 50 μm pin hole were used to obtain the Raman spectra from each grid point. The relative amount of adhered carbon at each point was represented by the area intensity of the Raman shift in the region from 900 to 1800 cm^{-1}, where the characteristic peaks from carbon including G- and D-peaks appeared.

3. Results

3.1 Results of friction and wear measurements

The transition of the friction coefficient between the PTFE composites and FC250 disk in both hydrogen and ambient air is compared in Fig.3. To confirm the repeatability of the friction and wear evaluations, a sliding test with an FC250 disk was performed twice in hydrogen. Pure PTFE showed an excessive wear under the sliding condition used in this study. Therefore, the sliding test of unfilled PTFE was disrupted at approximately 1500 m of sliding. The friction coefficient obtained just before terminating the experiment was used as the representative value for the unfilled PTFE friction in hydrogen, and it is indicated as a dotted line in each graph as a reference.

Reasonable repeatability of friction measurement was confirmed for the prepared single-filler PTFE composites except the GF-filled PTFE, which exhibited unstable fluctuations in the friction coefficient throughout the sliding test and inconsistent results in two experiments in hydrogen. Because the results of the friction measurement for the GF-filled PTFE were unstable, the difference between the hydrogen gas environment and ambient air was unclear. The two CF-filled PTFE composites showed similar results in the friction measurement, and the difference between hydrogen and air was conspicuous; the friction coefficient in hydrogen was much smaller than that in air. In addition, the friction coefficient of the CF-filled PTFE composites in hydrogen was lower than that of unfilled PTFE. Meanwhile, the PPS-filled PTFE showed almost identical results in both hydrogen and air. The frictional characteristic of the PPS-filled PTFE was similar to that of pure PTFE despite the difference in the surrounding environment.

The results of the friction measurement with the WC disk are shown in Fig. 4. The friction of the GF-filled PTFE became relatively stable with WC even though it began fluctuating in hydrogen at approximately 17000 m of sliding. However, the difference between hydrogen and air was relatively small for the friction coefficient of the GF-filled PTFE. By sliding against the WC disk, the difference between the pitch-CF and PAN-CF became clear in the friction measurement. The friction coefficient of the pitch-CF-filled PTFE is still lower in hydrogen compared with that in air; however, the gap between the two environments became much smaller compared with the results with FC250. Meanwhile, the effect of the gaseous environment on the frictional behaviour of the PAN-CF-filled PTFE was prominent. It resulted in a high and unstable friction in ambient air, whereas the friction coefficient decreased rapidly after the sliding test started and then stabilised at a low level of approximately 0.04 in hydrogen. The PPS-filled PTFE indicated a similar frictional behaviour to the WC disk and FC250; the difference between hydrogen and air was limited, and the friction coefficient value was similar to that of pure PTFE.

The specific wear rates of the composite pin specimens sliding against FC250 and WC are compared in Figs. 5 and 6, respectively. A small variation in the wear data can be identified by comparing the results of two series of

experiments in hydrogen using the FC250 disk. However, the variation was sufficiently small for discussing the contribution of filler materials and the effect of the hydrogen gas environment on the wear characteristics. As mentioned previously, the wear of pure PTFE was significant, and its wear rate was derived from the wear amount from the shortened sliding distance.

All filler materials effectively improved the wear resistance of PTFE, and the wear rates of the PTFE composites were less than those of unfilled PTFE with both disk materials. The result of the sliding test against the FC250 disk indicated that the wear rates of the GF-filled PTFE and pitch-CF-filled PTFE were larger in hydrogen compared with those in ambient air. The wear rate of the PPS-filled PTFE was similar in both hydrogen and air; meanwhile, the wear rate of the PAN-CF-filled PTFE in hydrogen was less than that in air, and it was the smallest among all materials and environments. Although the sliding counterface was changed from FC250 to WC, the effect on the wear rate of the GF-filled and PPS-filled PTFE was limited, and similar results as that of FC250 disk were obtained in both hydrogen and air. However, the counterface material imposed a certain effect on the wear rate of the CF-filled PTFE composites. The wear rate of CF-filled PTFE composites with the WC disk in air was higher than that with the FC250 disk, and the effect was more significant for the PAN-CF-filled PTFE. Consequently, the wear rates of the CF-filled PTFE composites sliding against WC, particularly that of the PAN-CF-filled PTFE, were smaller in hydrogen compared with those in ambient air.

The wear amounts of the FC250 and WC disks are compared in Figs. 7 and 8, respectively. The arrows in these figures indicate a negative value of the wear amount, i.e. the weight gain of the disk specimens by a material adhesion from the polymer pins. The wear amount of the FC250 disks became significantly higher in the GF-filled PTFE compared with those of other PTFE composites. In particular, the disk wear amount increased significantly in hydrogen. A significant wear amount in the FC250 disk was exhibited in the pitch-CF and PPS in hydrogen. However, a certain inconsistency was discovered in the first and second experiments. The wear amount of the WC disks was small compared with that of the FC250 disk. Only the WC disk that slid against the PPS-filled PTFE in air indicated a relatively large wear amount; however, the value was small when considering the large specific weight of WC.

For each PTFE composite pin, the results of friction and wear measurements are summarised in Fig. 9. The average of friction coefficient during the last 1000 m of sliding was used as a representative value of the composite friction in this figure. The distinct response to the hydrogen gas environment was clearly revealed for each filler material. The wear of the GF-filled PTFE was larger in hydrogen compared with that in air; however, the effect of

the environment on its friction was unclear. Meanwhile, the friction of the pitch-CF-filled PTFE was lower in hydrogen than in air, but the environmental effect on its wear was depended on the disc material. The response of the PAN-CF-filled PTFE was the most significant; its friction and wear were clearly lower in hydrogen than in air. Meanwhile, the friction and wear of the PPS-filled PTFE were insensitive to the environment since all data for it were assembled closely together.

3.2 Characterisation of composite worn surface

3.2.1 Morphology of composite worn surface

Representative worn surface images of PTFE composites are shown in Figs. 10–12. The effect of the hydrogen gas environment can be confirmed in the worn surface morphology of the GF-filled PTFE; the composite surface was roughened with some scratches and distortions in hydrogen, whereas it became relatively smooth in air (Fig.10). The difference between the hydrogen gas environment and ambient air was apparent in the worn surface morphology of the CF-filled PTFE composites, particularly when they slid against the WC disk. A smooth and greyish tribofilm was formed on the surface of the CF-filled PTFE composites in hydrogen (Figs. 11(a), (c)). A similar tribofilm formation in hydrogen was observed in the PAN-CF-filled PTFE with the FC250 disk (Fig. 11(e)). The formation of a greyish tribofilm on the surface of the CF-filled PTFE composites was a distinct characteristic of the hydrogen gas environment and was not observed in air (Figs. 11(b), (d), (f)). Furthermore, worn surface images of PPS-filled PTFE suggested the presence of a tribofilm too (Fig. 12). However, the difference thereof between hydrogen and air was insignificant.

3.2.2 Raman analysis of tribofilm

The tribofilm formation on the surface of the CF-filled PTFE composites was confirmed by Raman analysis. Raman spectra obtained from the worn surface of the CF-filled PTFE composites are compared in Fig. 13. For all measurements, the excitation laser spot was focused on the PTFE resin area, well away from the embedded CFs. The Raman spectra shown in Fig. 13 (a) were obtained from the greyish tribofilm formed on the worn surface of the pitch-CF-filled PTFE, which slid against the WC in hydrogen. The spectrum captured using the 20X objective lens exhibited typical PTFE peaks at 1382, 1303 1222, 735, 387, and 292 cm^{-1} in addition to broad but strong carbon G and D peaks approximately 1590 and 1350 cm^{-1}, respectively. However, if the objective lens was changed to 100X, the PTFE peaks vanished and two broad carbon peaks became predominant in the Raman spectrum. By increasing the magnification of the objective lens, the penetration depth of the excitation laser can be reduced and

information regarding the outermost surface layer can be obtained with a reduced background from the bulk. Therefore, these Raman spectra indicate the formation of a thin carbon film on the bulk PTFE resin. Similar results of Raman analysis were obtained for the PAN-CF-filled PTFE slid against WC in hydrogen (Fig. 13 (b)). With the FC250 disk, the intensity of the carbon peaks decreased to a low level; however, they were visible only for the PAN-CF-filled PTFE tested in hydrogen (Fig. 13 (c)). Characteristic carbon film formation in hydrogen can be confirmed by comparing the Raman spectra with the pin surface worn in air. The Raman spectra contained only peaks corresponding to PTFE (Fig. 13 (d)).

Carbon film formation could not be observed on the worn surface of the GF-filled PTFE (data not shown). Furthermore, Raman analysis was performed on the worn surface of the PPS-filled PTFE. However, strong fluorescence was emitted, and it was difficult to obtain a meaningful Raman spectrum. This might be because the tribofilm on the worn surface of the PPS-filled PTFE contained the PPS molecule and its fragments, and the benzene rings in the molecular structure emitted strong fluorescence.

3.3 Characterisation of sliding track formed on disk surface

3.3.1 Track formation on disk surface

After all experiments had been completed, the PTFE composites left a visible track on the sliding counterface. Macroscopic images of sliding tracks left on disk surfaces are shown in Figs. 14, 15, and 16. The PAN-CF-filled PTFE showed many similarities with the pitch-CF-filled PTFE in the macroscopic morphology of the remaining sliding tracks. Therefore, the corresponding images of the PAN-CF are not shown. The boldest sliding track with some abrasive grooves was left on the FC250 disks by the GF-filled PTFE, and apparent differences between the two test environments were indicated by its morphology (Figs. 14 (a), (b)). The sliding track formed in hydrogen exhibited characteristic white patches and deep grooves, whereas it became relatively flat in air. Furthermore, the GF-filled PTFE left a clear sliding track on WC disks too. However, it was less bold, and the influence of the test environments was indistinctive on WC (Figs. 14 (c), (d)). Moreover, the pitch-CF-filled PTFE left a clearly visible track on the FC250 disk; however, the track formation was limited to WC. A sliding track left by the PPS-filled PTFE was smooth and thin even on FC250, and they became significantly thinner on WC. For the CF- and PPS-filled PTFE composites, the effect of the test environment on the macroscopic observation of the sliding tracks was insignificant.

The microscopic images of sliding tracks formed on the FC250 disk are summarised in Fig. 17. They revealed more details regarding material adhesion and surface damage in the sliding tracks. Not only the GF-filled PTFE, but also the pitch-CF-filled PTFE roughened the FC250 surface with adhered materials and some scratches in hydrogen, whereas the disk surface became relatively smooth in air. Compared with the pitch-CF, the PAN-CF caused less damage to the FC250 surface in hydrogen; however, the formation of abrasive tracks was still obvious compared with that in air. The PPS-filled PTFE caused less damage on the disk surface compared with the other composites, and the disk surface was relatively smooth in both hydrogen and air.

3.3.2 Chemical analysis for sliding track

The XPS spectra obtained from the sliding track on the FC250 disk are shown in Fig. 18. The XPS signals obtained from the WC disks were unexpectedly weak and therefore excluded from the chemical analysis in this study. Because the transfer film formation from PTFE composites was emphasised, detailed spectra of fluorine (F1s) and carbon (C1s) were compared along with the oxygen spectrum (O1s). Only the GF-filled PTFE, silicon (Si2p), and calcium (Ca2p) spectra were supplemented for the analysis.

In most cases, the F1s spectra contained two large peaks: one at 688 eV was assigned to C–F bonds in adhered PTFE molecules and another peak at approximately 684 eV, indicating the presence of metal fluoride. Furthermore, a signal peak from C–F bonds also appeared in the C1s spectra at 291 eV. However, the C–F peaks in F1s and C1s disappeared completely after 20 s of argon ion etching. Another major peak in the carbon spectra was located at 284 eV, which was attributed to C–C bonds in the adhered carbon materials. Before argon ion etching, a metal hydroxide peak appeared at approximately 532 eV in the O1s spectrum, particularly from sliding tracks formed in hydrogen. The peak position in O1s was shifted to approximately 530 eV after argon etching, indicating the presence of metal oxides.

Owing to the sliding tracks formed by the GF-filled PTFE (Figs. 18 (a), (b)), strong PTFE and metal fluoride peaks appeared in the F1s spectrum. The presence of a certain amount of PTFE was confirmed by another PTFE peak in the C1s spectrum, accompanied by a much stronger C–C peak. In addition, the Ca2p spectrum had a calcium fluoride peak at 348 eV and a calcium carbonate peak at 351 eV, whereas no clear peak was observed in the Si2p spectrum. These characteristics in the XPS spectra appeared in both the hydrogen environment and ambient air. However, the sliding track formed in air had an extremely strong metal oxide peak, which indicated severe oxidation on the disk surface within the sliding track.

In the CF-filled PTFE composites (Figs. 18 (c), (d), (e), and (f)), the fluorine signals from the sliding track weakened compared with the GF- and PPS-filled PTFE composites. Particularly for the tracks formed in hydrogen, the intensity of the PTFE peak was extremely low in F1s, and it was buried in a background signal in the C1s spectrum. However, the intensity of the C–C peak in the C1s spectrum enhanced significantly in hydrogen. This peak was difficult to remove by argon ion etching, similar to the metal fluoride peak in the F1s spectrum. It was still visible even after 340 s of etching. This implies that this strong C–C signal was related to carbon materials that firmly adhered to the disk surface, not to contaminants attached during the storage period. Such a characteristic peak from adhered carbon was observed only in hydrogen and not observed in air. Compared with the pitch-CF, the PAN-CF-filled PTFE deposited a limited amount of materials on the sliding counterface, particularly in air, and both fluorine and carbon signals from the sliding track were week. However, the metal fluoride formation and carbon adhesion in hydrogen were almost comparable to those of the pitch-CF-filled PTFE.

In the case of the PPS-filled PTFE (Figs. 18 (g), (h)), the F1s spectra exhibited conspicuous PTFE and metal fluoride peaks. The intensity of the metal fluoride peak in F1s was relatively strong in hydrogen, whereas that of the PTFE peaks in both F1s and C1s became significantly stronger in air. Meanwhile, the intensity of the C–C peak in C1s was relatively small in both environments.

3.3.3 PTFE and carbon mapping in sliding track

A comparison of mapping images of PTFE within sliding tracks formed by CF- and PPS-filled PTFE composites is shown in Fig. 19. In the case of the CF-filled PTFE composites, the PTFE adhesion within the sliding track was not observed in hydrogen (Figs. 19(a), (c)), whereas the sliding track was partially covered with adhered PTFE in air (Figs. 19(b), (d)). Meanwhile, the sliding track formed by the PPS-filled PTFE was fully covered with a PTFE film both in hydrogen and air, even though the thickness of the adhered PTFE film was limited in hydrogen compared with that in air (Figs. 19 (e), (f)).

The results of carbon mapping (Fig. 20) were completely opposite to those of PTFE mapping. The sliding track formed by the CF-filled PTFE composites was fully covered with carbon deposited from the composites in hydrogen (Figs. 20(a), (c)). However, carbon deposition was not observed in air (Figs. 19(b), (d)). Such a significant carbon adhesion was a distinctive result of the CF-filled PTFE composites and was not observed on sliding tracks formed by the PPS-filled PTFE (Figs. 19(e), (f)) and GF-filled PTFE (data not shown) in hydrogen. The characteristics of the mapping images described above were mostly consistent with the results of the XPS analysis of the sliding tracks.

4. Discussion

In this study, four single-filler PTFE composites with different filler materials were prepared, and their friction and wear were evaluated in both ambient air and high-purity hydrogen gas to identify the tribological function of filler materials and the effect of the hydrogen gas environment on them. The results of the sliding test and subsequent surface characterisations indicated that each of the filler materials behaved differently in gaseous hydrogen; consequently, each PTFE composite showed a characteristic response to the sliding test environment. The friction and wear behaviour of the PTFE composites were mainly affected by two factors: the difference in the abrasiveness of hard fillers and the difference in tribofilm formation on the sliding surfaces.

The hydrogen gas environment showed an adverse effect on the wear behaviour of the GF- and pitch-CF-filled PTFE composites. Their wear rates were higher in hydrogen compared with those in air, especially when FC250 disks with relatively low hardness were used as a sliding counterface. The increased wear rate of these composites in hydrogen was coupled with severer surface damages of the disk specimens. The increased damage of sliding counterface was confirmed by the increased wear amount of disk specimens in hydrogen. On the other hand, the PAN-CF and PPS did not result in such an increase in disk surface damage and a correspondingly large composite wear in the hydrogen gas environment.

To compare the mechanical properties of the two CF fillers used in this study, a smooth cross-section of the CF-filled PTFE composites was prepared, and an indentation test was performed on flat CF end-faces exposed in the cross-section using a nanoindenter (UNHT, Anton-Paar). The Vickers hardness of the pitch-CF and PAN-CF obtained via the indentation test were 243 and 97, respectively; it was revealed that the pitch-CF was 2.5 times harder than the PAN-CF. Therefore, the difference between the two CF-filled PTFE composites can be explained by the difference in the fibre hardness. The sliding test results indicate that the abrasiveness of hard fibres, GF, and pitch-CF, intensified and resulted in more damage on the disk surfaces in gaseous hydrogen than in air.

The limited amount of oxygen and water in the hydrogen gas environment can be considered as a primary factor for the increased counterface damage caused by the hard fibres. The results of the XPS analysis indicated that the surface of the FC250 disks that slid against GF- or pitch-CF-filled PTFE composites in air contained a certain amount of metal oxide (Figs. 18 (b), (d)). This metal oxide in the surface region might provide protection against abrasive wear by hard fillers. However, the residual water content of the hydrogen gas environment was maintained at less than 10 ppm in this study. In such a high-purity gas environment, the reformation of a protective

metal oxide layer on the disk surface should be reduced after the removal of the initial surface oxide layer. In addition, hydrogen reduction might contribute to a decrease in the amount of protective metal oxides on the disk surface. Nakashima et al. experimentally revealed that the hydrogen gas environment can decrease the thickness of the oxidised passive layer on a stainless steel surface and produce metal hydroxides under the high-pressure and high-temperature conditions [37]. Although the sliding test in hydrogen was conducted under atmospheric pressure in this study, the local contact pressure should be high and provide sufficient energy for hydrogen reduction to be applied by sliding at the asperity contact area. In fact, the XPS analysis suggested metal hydroxide formation for the sliding track formed in hydrogen. The limited metal oxide formation in hydrogen was confirmed in the XPS spectra (Figs. 18 (a), (c)) for sliding tracks formed by the GF- and pitch-CF filled PTFE composites. FC250 disks with relatively low hardness and decreased surface oxide layer were more susceptible to abrasive wear by the hard fibre in PTFE composites.

Using a hard WC disk as a sliding counter face, the effect of intensified fibre abrasion in the high-purity hydrogen was tolerated well and the wear increase of the GF- and Pitch-CF-filled PTFE composites in hydrogen was mitigated. The detrimental effect of the enhanced fibre abrasion in hydrogen also could be tolerated well by reducing the hardness of the reinforcing fibre. The low hardness PAN-CF did not cause such a severe surface damage even on the FC250 disk in hydrogen. If the effect of fibre abrasion is negligibly small, then the hydrogen gas environment results in a favourable effect on the friction and wear of the CF-filled PTFE composites. In this case, the distinct effect of hydrogen appeared in the tribofilm formation on the sliding surfaces.

The friction coefficient and wear rate of the pitch-CF-filled PTFE decreased in hydrogen compared with that in air if it slid against WC disk. In addition, the PAN-CF filled PTFE showed much better friction and wear in hydrogen than in air regardless of the disk material. For both composites, the XPS analysis revealed clear differences in the chemical composition of the transfer film formed on the FC250 disk surface between the two test environments. In ambient air, the transfer film mainly comprised PTFE, metal fluoride, and some oxides. Although the underlining metal fluoride and metal oxide were firmly bonded to the disk surface and remained even after 340 s of argon ion etching, the PTFE and its fragments in the uppermost surface were easily removed and could not be identified after etching for 20 s. Meanwhile, the amount of PTFE in the transfer film was limited in hydrogen. Furthermore, the transfer film formed in the hydrogen environment contained a significant amount of carbon, which was indicated by the strong XPS signal appearing around 284 eV in the C1s spectrum, in addition to metal fluoride and oxides. This carbon constituent of the transfer film adhered to the disk surface firmly together with

metal fluoride and remained after 340 s of etching, unlike the PTFE adhered in air. The source of this carbon should be CFs contained in the composites, as the corresponding carbon constituent was not observed in the transfer films formed by the GF- and PPS-filled PTFE. The significant effect of the high-purity hydrogen environment on the transfer film formation of the CF-filled PTFE composites described above was supported by the FT-IR and Raman mapping images. A certain area of the sliding tracks was covered with adhered PTFE, and the carbon adhesion was negligible in air. However, the adhered PTFE disappeared, and the sliding tracks were fully covered with adhered carbon in hydrogen.

During the sliding in hydrogen, the carbon-based tribo-film was also developed on the surface of CF-filled PTFE composites, as indicated by Raman analysis. The carbon film on the composite surface might be formed from fine carbon wear particles released from the CF worn surfaces. It covered the PTFE resin area in the sliding surface and interrupted the subsequent deposition of PTFE on the disk surface by reducing the direct contact between the PTFE resin and the sliding counterface. Consequently, sliding was exerted at the interface between the carbon-based tribofilms on the composite surface and the carbon-rich transfer film on the disk surface in hydrogen. As suggested by previous researchers, the characteristics of tribofilms formed on sliding surfaces govern the tribological behaviour of polymer composites [17][18][50][51][52]. The carbon tribofilms formed in high-purity hydrogen gas had an excellent low friction property, and the friction coefficient of the CF-filled PTFE composites was always lower in hydrogen compared with that in air. The friction coefficient decreased to 0.04 for the PAN-CF-filled PTFE sliding against the WC disk. It was the minimum value of the friction coefficient obtained in this study and significantly lower than the friction coefficient of unfilled PTFE under the same test settings (0.33). The lubrication effect of the carbon tribofilms reduced the wear of the PTFE composite when the surface abrasion by the CF was insignificant. The wear rate of the PAN-CF-filled PTFE sliding against WC became 70 times lower in hydrogen than in air.

The formation of the carbon tribofilm was facilitated in the high-purity hydrogen gas, likely because of the limited amount of water and oxygen molecules. Water and oxygen in air might oxidise some of fine carbon wear particles or clump them together and assist the exclusion of wear particles from the sliding interface. If the water and oxygen contents of the sliding test environment are reduced considerably, then a larger amount of carbon wear particles will be trapped in the sliding interface and assembled together to form the tribofilms on both the sliding counterface and the composite surface. Furthermore, the chemical function of hydrogen might contribute to carbon tribofilm formation. However, many uncertainties remain regarding the mechanism of carbon tribofilm formation

in high-purity hydrogen. Further studies are necessary to understand the relationship between the amount of residual water/oxygen in hydrogen and the development of carbon tribofilm, as well as the chemical or physical interactions between hydrogen and carbon in the sliding interface.

Whereas the tribological behaviour of the CF-filled PTFE composites was highly depended on the sliding test environment, the friction and wear of the PPS-filled PTFE was insensitive to the surrounding hydrogen and demonstrated consistent results in both test environments, as indicated in Fig. 9 (d). This was because the abrasiveness of PPS was limited compared with that of the CF, and also the tribofilm formation on the sliding surfaces was not susceptible to the high-purity hydrogen gas environment. The results of XPS analysis indicated that the transfer film formed on the disk surface had similar chemical compositions for the two test environments, and that the main constituent was PTFE for the PPS-filled PTFE, although the amount of deposited PTFE was much larger in air. Consequently, the friction between the composite and the sliding counterface was governed by the shear resistance of the PTFE-based transfer film and unaffected by the test environment. As such, the friction coefficient of the PPS-filled PTFE was similar to that of the unfilled PTFE in both hydrogen and air.

Short fibre reinforcement with GF, CF, and other strong fibres has been used to improve the mechanical strength and the load-bearing capacity of polymer composites [15][53][55][56]. It is also an effective method to improve the wear resistance while remaining or even increasing the friction coefficient in some cases [56]. Therefore, it is often supplemented with another filler with a low shear strength to reduce friction in actual applications. From the viewpoint of friction, CFs are more advantageous over GFs because they can form a transfer film and demonstrate a certain self-lubricity for maintaining low friction [57][58]. The results of this study highlighted that the self-lubricity of CFs can be emphasised by the high-purity hydrogen by encouraging carbon-based tribofilm formation. The sliding test conditions in this study were defined to simulate a piston ring used in a reciprocating hydrogen gas compressor. Therefore, GFs are not an ideal material for the fibre reinforcement of the piston ring material, as wear might increase owing to the enhanced abrasion by GFs in hydrogen. Short fibre reinforcement with CFs of sufficiently low hardness is a preferable choice for this application. CFs can not only improve the mechanical strength, but also reduce the friction and wear of piston rings through the distinct lubricity of carbon tribo-film.

Some hard particles have been incorporated into polymer composites as a filler to improve wear resistance [15][59][60][61][62]. Briscoe and Yao demonstrated that the wear rate of PTFE composites reduced significantly by adding 20 wt% hard PEEK particles [59]. They explained that the composite wear was reduced because most of

the contact load was supported by high wear-resistant PEEK particles at the sliding interface, whereas low friction was maintained by the transfer film formed from PTFE resin. PPS is a type of engineering plastic with high chemical stability and excellent high-temperature performance [63][64]. It also exhibits high wear resistance and has been used as a hard particle filler in PTFE composites. In this study, the tribological function of PPS was not affected in the high-purity hydrogen gas, and the PPS-filled PTFE demonstrated favourable wear resistance as well as moderate friction by the PTFE transfer film in both air and hydrogen. Therefore, PPS can be considered as another suitable filler material for piston rings used in hydrogen gas compressors.

5. Conclusions

All filler materials tested in this study improved the wear resistance of PTFE as a strengthening filler. However, the effect of the hydrogen gas environment differed for each filler material, and the friction and wear characteristics of PTFE composites in hydrogen differed depending on the incorporated filler. The major findings in this study are as follows:

1. The abrasiveness of hard GFs and CFs enhanced in the high-purity hydrogen gas environment, and PTFE composites filled with these hard fibres increased counterface damage and subsequently increased wear in high-purity hydrogen.

2. The high-purity hydrogen gas environment imposed a distinct influence on the tribofilm formation by the CF-filled PTFE. A carbon-rich transfer film was formed on the sliding counterface, whereas the sliding surface of the composite was covered with a carbon tribofilm in hydrogen. Consequently, the CF-filled PTFE demonstrated low friction and wear in the high-purity hydrogen when the fibre hardness was not too hard relative to the hardness of the sliding counterface.

3. The tribological function of the PPS was unaffected by hydrogen. The PPS-filled PTFE formed sufficient amount of PTFE transfer film on the sliding counterface and maintained low friction and wear in high-purity hydrogen as well as in air.

Acknowledgement

The authors would like to thank Mr. Y. Naganuma for his great assistance in our experiments. Part of this study was conducted in the program, “Research and Development of Technology for Hydrogen Utilization” funded by New Energy and Industrial Technology Development Organization (NEDO.).

References

[1] Staffell I, Scamman D, Velazquez Abad A, Balcombe P, Dodds PE, Ekins P, Shah N, Ward KR. The role of hydrogen and fuel cells in the global energy system. Energy Environ Sci 2019;12:463–91. https://doi.org/10.1039/c8ee01157e.

[2] Turner JA. Sustainable Hydrogen Production. Science 2004;305:972–4. https://doi.org/10.1016/b978-0-444-64203-5.00001-0.

[3] Sugimura J. Overview of tribology researches for high-pressure hydrogen systems. Tribol Und Schmierungstechnik 2019;66:24–32.

[4] Eberle U, Müller B, Von Helmolt R. Fuel cell electric vehicles and hydrogen infrastructure: Status 2012. Energy Environ Sci 2012;5:8780–98. https://doi.org/10.1039/c2ee22596d.

[5] Nonobe Y. Development of the fuel cell vehicle mirai. IEEJ Trans Electr Electron Eng 2017;12:5–9. https://doi.org/10.1002/tee.22328.

[6] Li M, Bai Y, Zhang C, Song Y, Jiang S, Grouset D, Zhang M. Review on the research of hydrogen storage system fast refueling in fuel cell vehicle. Int J Hydrogen Energy 2019;44:10677–93. https://doi.org/10.1016/j.ijhydene.2019.02.208.

[7] Rothuizen E, Mérida W, Rokni M, Wistoft-Ibsen M. Optimization of hydrogen vehicle refueling via dynamic simulation. Int J Hydrogen Energy 2013;38:4221–31. https://doi.org/10.1016/j.ijhydene.2013.01.161.

[8] Reddi K, Elgowainy A, Sutherland E. Hydrogen refueling station compression and storage optimization with tube-trailer deliveries. Int J Hydrogen Energy 2014;39:19169–81. https://doi.org/10.1016/j.ijhydene.2014.09.099.

[9] ISO14687-2. Hydrogen fuel — Product specification — Part 2:Proton exchange membrane (PEM) fuel cell applications for road vehicles. 2012.

[10] Blackwell JW. PTFE Seals in Reciprocating Compressors. The American Society of Mechanical Engineers; 1975.

[11] Radcliffe C. Sealing developments for reciprocating gas compressors. Sealing Technology 2005;2005:7-11. https://doi.org/10.1016/S1350-4789(05)70872-2

[12] Flitney R. Seals and Sealing Handbook. 6th ed.: Butterworth-Heinemann; 2014. https://doi.org/10.1016/C2012-0-03302-9.

[13] Yang XB, Jin XQ, Du ZM, Cui TS, Yang SK. Experimental study on frictional and sealing performances of packing rings in an oil-free gas compressor. J Shanghi Jiaotong University 2009;14:725–31. https://doi.org/10.1007/s12204-009-0725-8.

[14] Yu W, Dianbo X, Jiannei F, Zueyuan P. Research on sealing performance and self-acting valve reliability in high-pressure oil-free hydrogen compressors for hydrogen refueling stations. Int J Hydrogen Energy 2010;35:8063–70. https://doi.org/10.1016/j.ijhydene.2010.01.089.

[15] Tanaka K. Effects of Various Fillers on the Friction and Wear of PTFE-Based Composites. In: Friedrich K, editor. Frict. Wear Polym. Compos., vol. 1, Elsevier; 1986, p. 137–74. https://doi.org/10.1016/B978-0-444-42524-9.50009-0.

[16] Blanchet TA, Kennedy FE. Sliding wear mechanism of polytetrafluoroethylene (PTFE) and PTFE composites. Wear 1992;153:229–43. https://doi.org/10.1016/0043-1648(92)90271-9.

[17] Burris DL, Santos K, Lewis SL, Liu X, Perry SS, Blanchet TA, Schadler LS, Sawyer WG. Polytetrafluoroethylene matrix nanocomposites for tribological applications. In: Friedrich K, Schlarb A, editors. Tribol. Polym. Nanocomposites Frict. Wear Bulk Mater. Coatings Second Ed., Butterworth-Heinemann; 2013, p. 571–617. https://doi.org/10.1016/B978-0-444-59455-6.00017-9.

[18] Harris KL, Pitenis AA, Sawyer WG, Krick BA, Blackman GS, Kasprzak DJ, Junk CP. PTFE Tribology and the Role of Mechanochemistry in the Development of Protective Surface Films. Macromolecules 2015;48:3739–45. https://doi.org/10.1021/acs.macromol.5b00452.

[19] Ding L, Axinte D, Butler-Smith P, Abdelhafeez HA. Study on the characterisation of the PTFE transfer film and the dimensional designing of surface texturing in a dry-lubricated bearing system. Wear 2020;448–449:203238. https://10.1016/j.wear.2020.203238.

[20] Valente CAGS, Boutin FF, Rocha LPC, do Vale JL, da Silva CH. Effect of Graphite and Bronze Fillers on PTFE Tribological Behavior: A Commercial Materials Evaluation. Tribol Trans 2020;63:356–70. https://doi.org/10.1080/10402004.2019.1695032.

[21] Li S, Duan C, Li X, Shao M, Qu C, Zhang D, Wang Q, Wang T, Zhang X. The effect of different layered materials on the tribological properties of PTFE composites. Friction 2020;8:542–52. https://doi.org/10.1007/s40544-019-0276-4.

[22] Sun W, Liu X, Liu K, Xu J, Wang W, Ye J. Paradoxical Filler Size Effect on Composite Wear: Filler–Matrix Interaction and Its Tribochemical Consequences. Tribol lett 2020;68:131. https://doi.org/10.1007/s11249-020-01375-w.

[23] Yang Y, Wang H, Ren J, Gao G, Zhao G, Chen S, Wang N, Wang J. Multi-environment adaptability of self-lubricating core/shell PTFE@PR composite: Tribological characteristics and transfer mechanism. Tribol Int 2021;154:106718. https://doi.org/10.1016/j.triboint.2020.106718.

[24] Ciruna JA, Szieleit HJ. The effect of hydrogen on the rolling contact fatigue life of AISI 52100 and 440C steel balls. Wear 1973;24:107–18. https://doi.org/10.1016/0043-1648(73)90207-X.

[25] Endo T, Dong D, Imai Y, Yamamoto Y. Study on rolling contact fatigue in hydrogen atmosphere: Improvement of rolling contact fatigue life by formation of surface film. Tribol Interface Eng Ser 2005;48:343–50. https://doi.org/10.1016/s0167-8922(05)80036-7.

[26] Tanaka H, Morofuji T, Enami K, Hashimoto M, Sugimura J. Effect of environmental gas on surface initiated rolling contact fatigue. Tribol Online 2013;8:90–6. https://doi.org/10.2474/trol.8.90.

[27] Donnet C, Grill A, Fontaine J, Le Mogne T, Lefebvre F, Patel V, Jahnes C. Fundamentals on the friction mechanism of diamondlike carbon films. Tribol Ser 1999;36:333–41. https://doi.org/10.1016/s0167-8922(99)80054-6.

[28] Erdemir A. The role of hydrogen in tribological properties of diamond-like carbon films. Surf Coatings Technol 2001;146–147:292–7. https://doi.org/10.1016/S0257-8972(01)01417-7.

[29] Fontaine J, Belin M, Le Mogne T, Grill A. How to restore superlow friction of DLC: The healing effect of hydrogen gas. Tribol Int 2004;37:869–77. https://doi.org/10.1016/j.triboint.2004.07.002.

[30] Okubo H, Oshima K, Tuboi R, Tadokoro C, Sasaki S. Effects of hydrogen on frictional properties of DLC films. Tribol Online 2015;10:1881–2198. https://doi.org/10.2474/trol.10.397.

[31] Nosaka M, Mifune A, Kawaguchi M, Shiiba T, Kato T. Friction fade-out at polymer-like carbon films slid by ZrO2 pins under hydrogen environment. Proc Inst Mech Eng Part J J Eng Tribol 2015;229:1030–8. https://doi.org/10.1177/1350650115569857.

[32] Berman D, Deshmukh SA, Sankaranarayanan SKRS, Erdemir A, Sumant A V. Extraordinary Macroscale Wear Resistance of One Atom Thick Graphene Layer. Adv Funct Mater 2014;24:6640–6. https://doi.org/10.1002/adfm.201401755.

[33] Berman D, Erdemir A, Sumant AV. Approaches for Achieving Superlubricity in Two-Dimensional Materials. ACS Nano 2018;12:2122–37. https://doi.org/10.1021/acsnano.7b09046.

[34] Fukuda K, Sugimura J. Sliding properties of pure metals in hydrogen environment. 2008 Proc. STLE/ASME Int. Jt. Tribol. Conf. IJTC 2008, 2009, p. 11–3.

[35] Fukuda K, Sugimura J. Influences of trace water in a hydrogen environment on the tribological properties of pure iron. Tribol Online 2013;8:22–7. https://doi.org/10.2474/trol.8.22.

[36] Tanaka H, Sawae Y, Fukuda K, Yamagami S, Morita T, Izumi N, et al. New Experiment System for Sliding Tests in Hydrogen and Surface Analysis with Transfer Vessel. Tribol Online 2009;4:82–7. https://doi.org/10.2474/trol.4.82.

[37] Nakashima K, Yamaguchi A, Kurono Y, Sawae Y, Murakami T, Sugimura J. Effect of high-pressure hydrogen exposure on wear of polytetrafluoroethylene sliding against stainless steel. Proc Inst Mech Eng Part J J Eng Tribol 2010;224:285–92. https://doi.org/10.1243/13506501JET642.

[38] Nosaka M, Kikuchi M, Oike M, Kawai N. Tribo-characteristics of cryogenic hybrid ceramic ball bearings for rocket turbopumps: Bearing wear and transfer film©. Tribol Trans 1999;42:106–15. https://doi.org/10.1080/10402009908982197.

[39] Nosaka M, Kikuchi M, Kawai N, Kikuyama H. Effects of iron fluoride layer on durability of cryogenic high-speed ball bearings for rocket turbopumps. Tribol Trans 2000;43:163–74. https://doi.org/10.1080/10402000008982326.

[40] Zhang Z, Klein P, Theiler G, Hübner W. Sliding performance of polymer composites in liquid hydrogen and liquid nitrogen. J Mater Sci 2004;39:2989–95. https://doi.org/10.1023/B:JMSC.0000025824.18291.f0.

[41] Theiler G, Gradt T. Friction and wear behaviour of polymers in liquid hydrogen. Cryogenics 2018;93:1–6. https://doi.org/10.1016/j.cryogenics.2018.05.002.

[42] Theiler G, Gradt T. Friction and wear behaviour of graphite filled polymer composites in hydrogen environment. Tribol Online 2015;10:207–12. https://doi.org/10.2474/trol.10.207.

[43] Theiler G, Gradt T. Tribological characteristics of polyimide composites in hydrogen environment. Tribol Int 2015;92:162–71. http://dx.doi.org/10.1016/j.triboint.2015.06.001.

[44] Theiler G, Gradt T. Environmental effects on the sliding behaviour of PEEK composites. Wear 2016;368–369:278–86. https://doi.org/10.1016/j.wear.2016.09.019.

[45] Theiler G, Gradt T. Influence of counterface and environment on the tribological behaviour of polymer materials. Polymer Testing 2021;93:106912. https://doi.org/10.1016/j.polymertesting.2020.106912

[46] Morita T, Sato F, Sawae Y, Sugimura J. Effects of metal counter surfaces on friction and wear of polymeric seal materials in hydrogen. BHR Gr. - 21st Int. Conf. Fluid Seal., 2011, p. 167–78.

[47] Sawae Y, Fukuda K, Miyakoshi E, Doi S, Watanabe H, Nakashima K, et al. Tribological characterization of polymeric sealing materials in high pressure hydrogen gas. Am. Soc. Mech. Eng. Tribol. Div. TRIB, 2010, p. 251–3. https://doi.org/10.1115/IJTC2010-41238.

[48] Sawae Y, Miyakoshi E, Doi S, Watanabe H, Kurono Y, Sugimura J. Friction and wear of bronze filled PTFE and graphite filled PTFE in 40 MPA hydrogen gas. Am. Soc. Mech. Eng. Tribol. Div. TRIB, 2011, p. 249–51. https://doi.org/10.1115/IJTC2011-61215.

[49] Jintang G. Tribochemical effects in formation of polymer transfer film. Wear 2000;245:100–6. https://doi.org/10.1016/S0043-1648(00)00470-1.

[50] Campbell KL, Sidebottom MA, Atkinson CC, Babuska TF, Kolanovic CA, Boulden BJ, Junk CP, Krick BA. Ultralow Wear PTFE-Based Polymer Composites - The Role of Water and Tribochemistry. Macromolecules 2019;52:5268–77. https://doi.org/10.1021/acs.macromol.9b00316.

[51] Alam KI, Dorazio A, Burris DL. Polymers Tribology Exposed: Eliminating Transfer Film Effects to Clarify Ultralow Wear of PTFE. Tribol Lett 2020;6:67. https://doi.org/10.1007/s11249-020-01306-9

[52] Cui W, Raza K, Zhao Z, Yu C, Tao L, Zhao W, Chen W, Peng S, Xu Q, Ma L, Hu Y, Liao D, Liang B, Wang T, Ma T. Role of transfer film formation on the tribological properties of polymeric composite materials and spherical plain bearing at low temperatures. Tribol Int 2020;152:106569. https://doi.org/10.1016/j.triboint.2020.106569.

[53] Huang R, Ma S, Zhang M, Yang J, Wang D, Zhang L, Xu, J. Wear evolution of the glass fiber-reinforced PTFE under dry sliding and elevated temperature. Materials 2019;12:1082. https://doi.org/10.3390/ma12071082.

[54] Funke HH, Grissom BL, McGrew CE, Raynor MW. Techniques for the measurement of trace moisture in high-purity electronic specialty gases. Rev Sci Instrum 2003;74:3909–33. https://doi.org/10.1063/1.1597939.

[55] HÄGER AM, Davies M. Short-Fibre Reinforced, High-Temperature Resistant Polymers for a Wide Field of Tribological Applications. In: Friedrich K, editor. Advances in Composite Tribology, Elsevier; 1993, p. 17-157. https://doi.org/10.1016/B978-0-444-89079-5.50008-8.

[56] Briscoe BJ, Sinha SK. Tribological applications of polymers and their composites - past, present and future prospects. In: Friedrich K, editor. Tribology of Polymeric Nanocomposites: Friction and Wear of Bulk Materials and Coatings: 2nd ed., Elsevier; 2013, p. 1-22. https://doi.org/10.1016/B978-0-444-59455-6.00001-5.

[57] Sharma M, Mohan Rao I, Bijwe J. Influence of fiber orientation on abrasive wear of unidirectionally reinforced carbon fiber-polyetherimide composites. Tribol Int 2010;43:959–64. https://doi.org/10.1016/j.triboint.2009.12.064.

[58] Bijwe J, Sharma M. Carbon Fabric-Reinforced Polymer Composites and Parameters Controlling Tribological Performance. In: Davim JP, editor. Wear of Advanced Materials; John Wiley and Sons; 2013, p. 1-60. https://doi.org/10.1002/9781118562093.ch1.

[59] Briscoe BJ, Yao LH, Stolarski TA. Friction and Wear of Poly(Tetrafluoroethylene)-Poly(Etheretherketone) Composities; an Initial Appraisal of the Optimum Composition. Wear 1986;108:357-74. https://doi.org/10.1016/0043-1648(86)90013-X

[60] Friedrich K, Lu Z, Hager AM. Recent advances in polymer composites' tribology. Wear 1995;190:139–44. https://doi.org/10.1016/0043-1648(96)80012-3.

[61] Haidar DR, Alam KI, Burris DL, Tribological Insensitivity of an Ultralow-Wear Poly(etheretherketone)-Polytetrafluoroethylene Polymer Blend to Changes in Environmental Moisture. J Phys Chem C 2018;122:5518–24. https://doi.org/10.1021/acs.jpcc.7b12487.

[62] Gao G, Gong J, Qi Y, Ren J, Wang H, Yang D, Chen S. Tribological Behavior of PTFE Composites Filled with PEEK and Nano-ZrO_2. Tribol Trans 2020;63:296–304. https://doi.org/10.1080/10402004.2019.1687796.

[63] Schwartz CJ, Bahadur S. The role of filler deformability, filler-polymer bonding, and counterface material on the tribological behavior of polyphenylene sulfide (PPS). Wear 2001;250:1532–40. https://doi.org/10.1016/S0043-1648(01)00799-2.

[64] Zuo P, Tcharkhtchi A, Shirinbayan M, Fitoussi J, Bakir F. Overall Investigation of Poly (Phenylene Sulfide) from Synthesis and Process to Applications—A Review. Macromol Meter Eng 2019;304:1800686. https://doi.org/10.1002/mame.201800686.

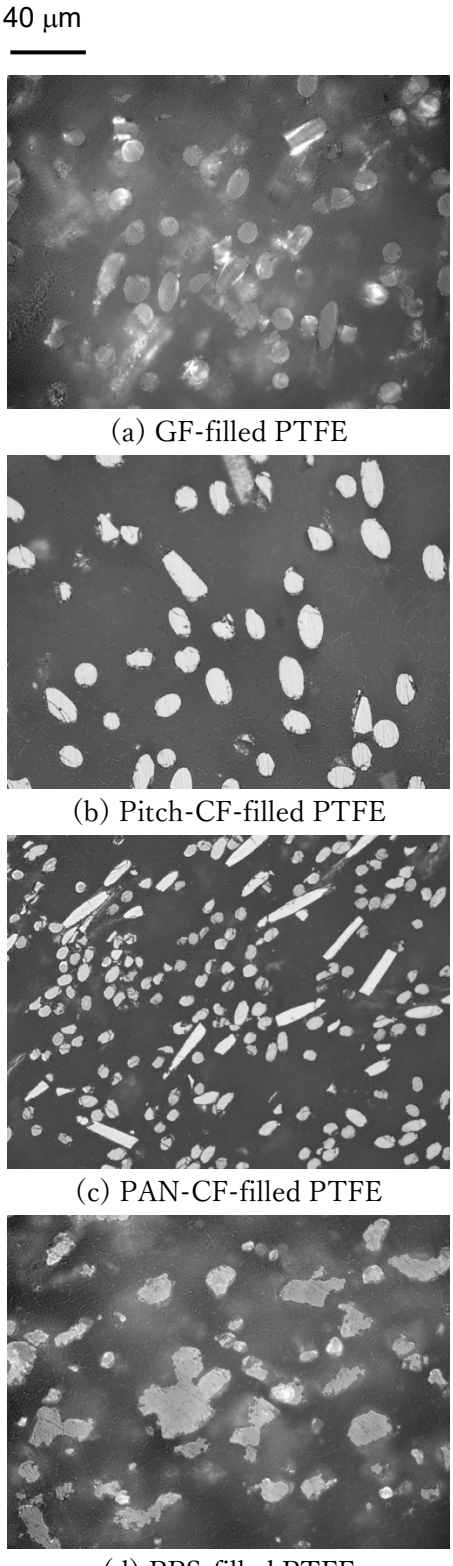

(a) GF-filled PTFE

(b) Pitch-CF-filled PTFE

(c) PAN-CF-filled PTFE

(d) PPS-filled PTFE

Fig.1 Cross section image of PTFE composites

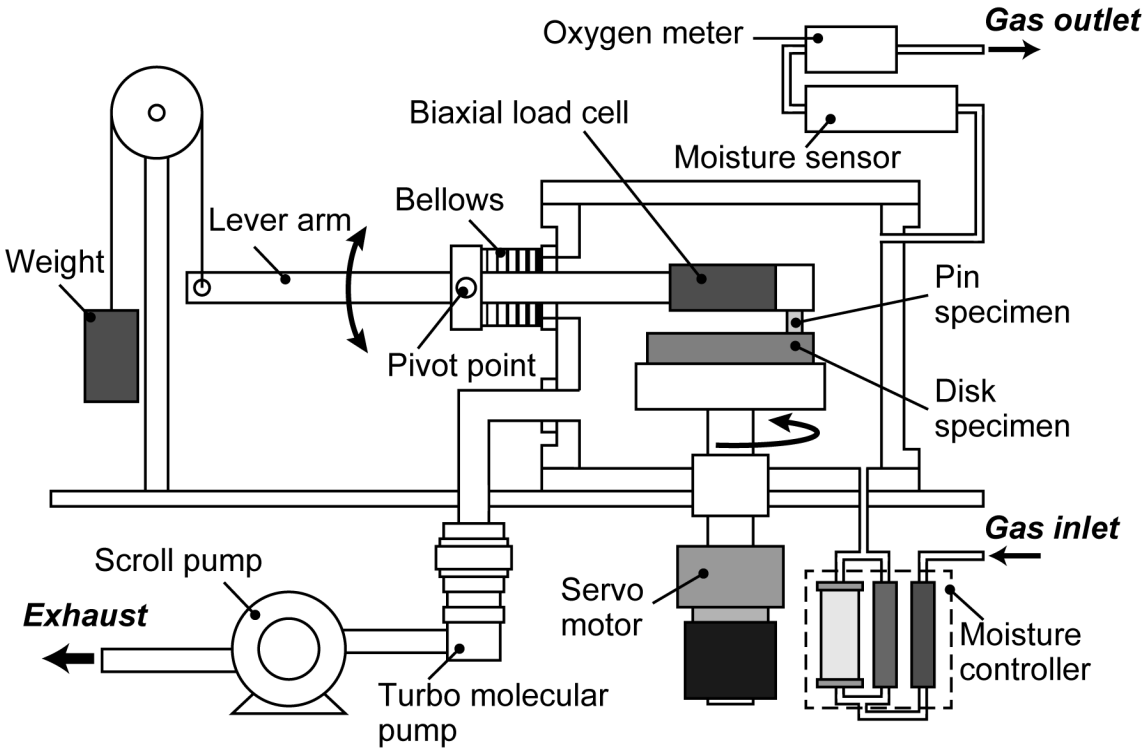

Fig.2 Schematic of Pin-on-Disk type tribometer installed in the high vacuum chamber

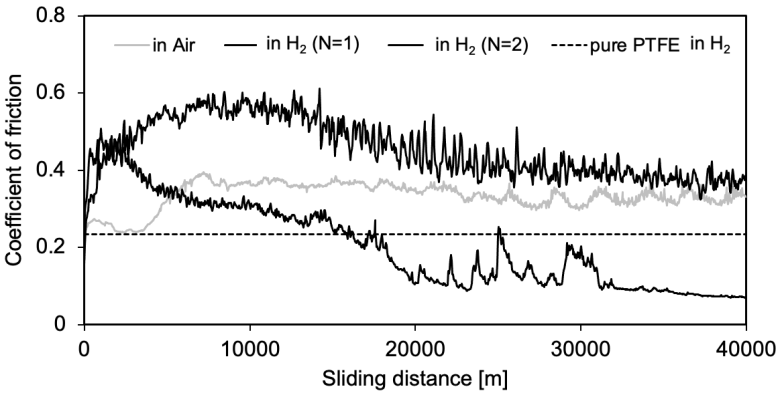

(a) GF-filled PTFE

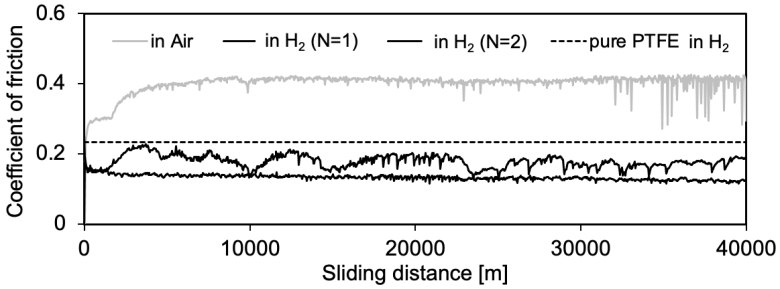

(b) Pitch-CF-filled PTFE

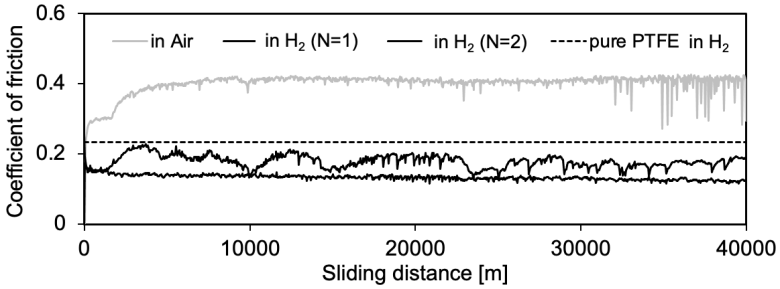

(c) PAN-CF-filled PTFE

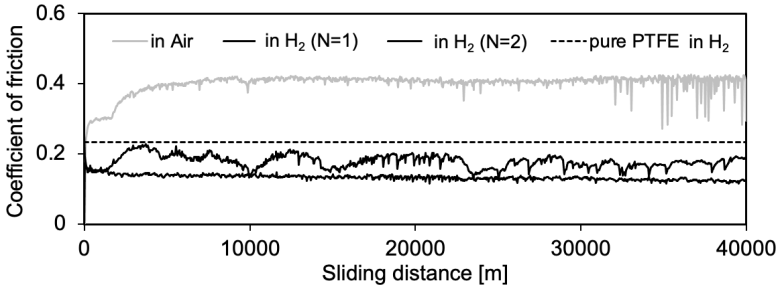

(d) PPS-filled PTFE

Fig.3 Transition of friction coefficient between PTFE composites and FC250 disk

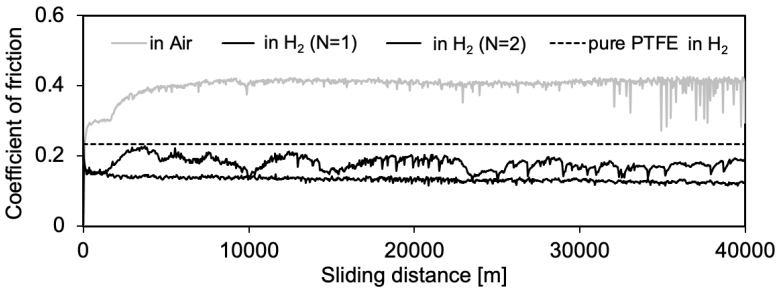

(a) GF-filled PTFE

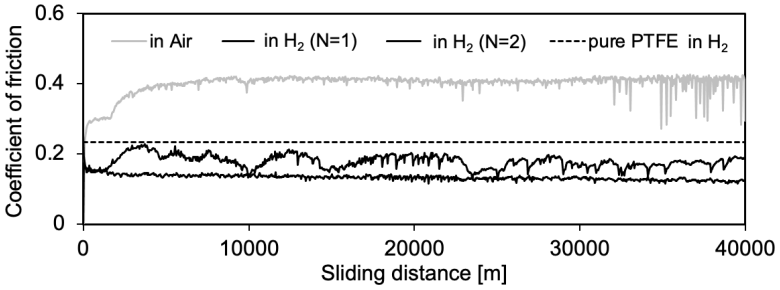

(b) Pitch-CF-filled PTFE

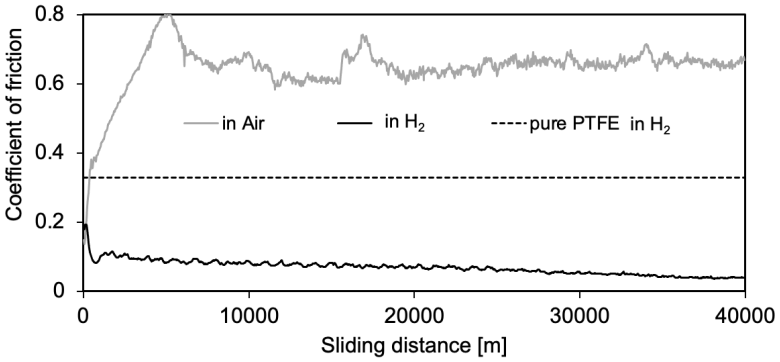

(c) PAN-CF-filled PTFE

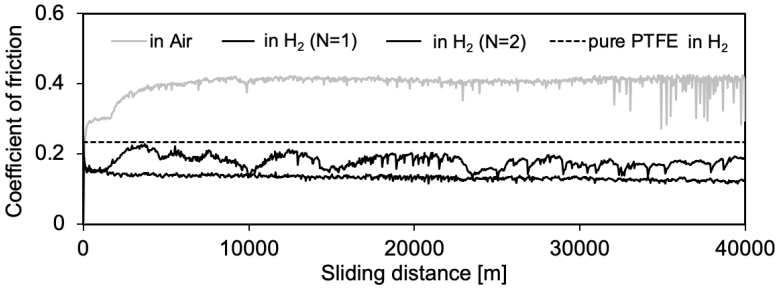

(d) PPS-filled PTFE

Fig.4 Transition of friction coefficient between PTFE composites and WC disk

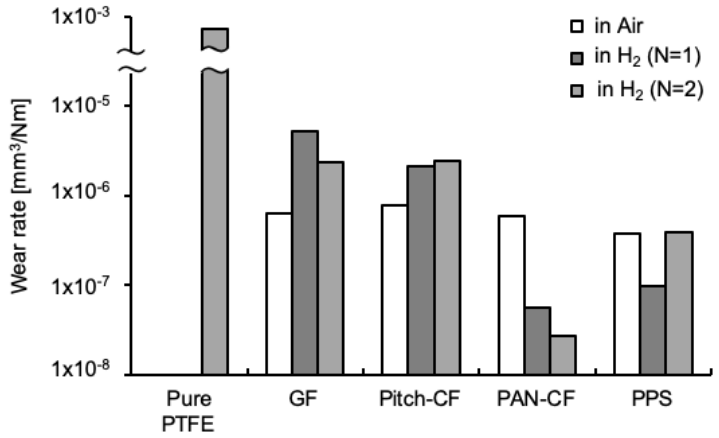

Fig.5 Comparison of specific wear rate of PTFE composite slid against FC250 disk

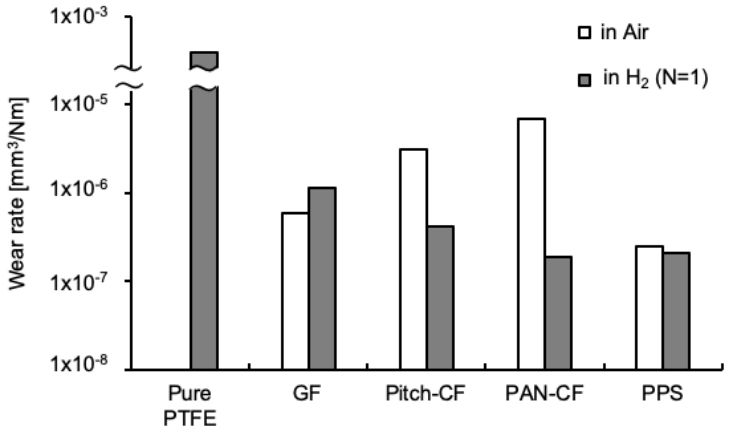

Fig.6 Comparison of specific wear rate of PTFE composite slid against WC disk

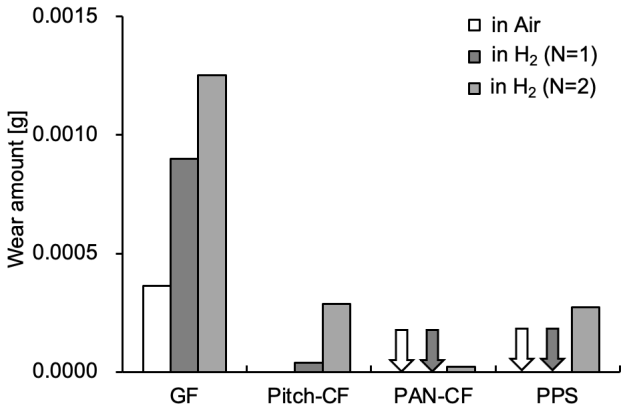

Fig.7 Wear amount of FC250 disk

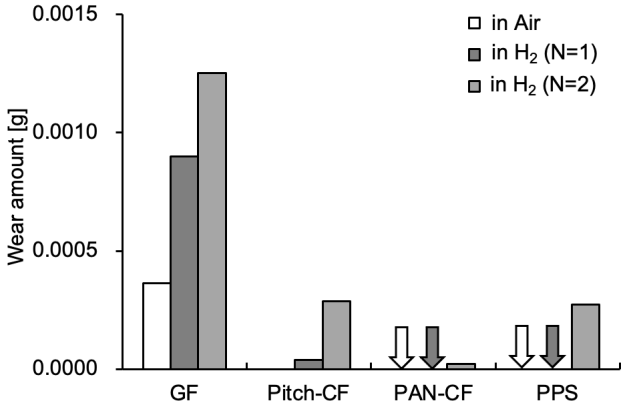

Fig.8 Wear amount of WC disk

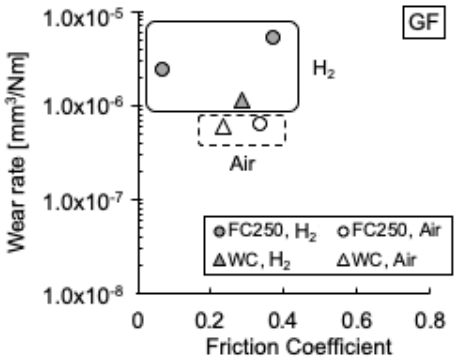

(a) GF-filled PTFE

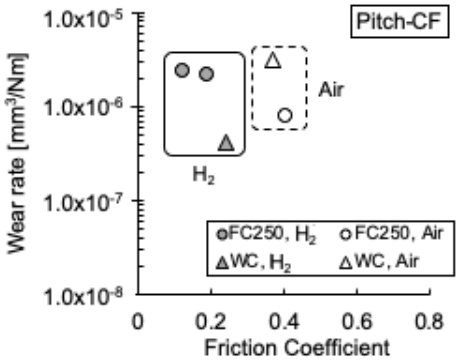

(b) Pitch-CF-filled PTFE

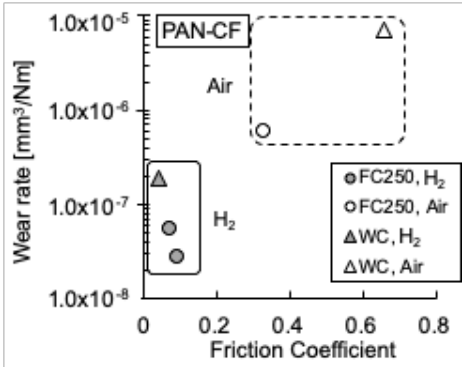

(c) PAN-CF-filled PTFE

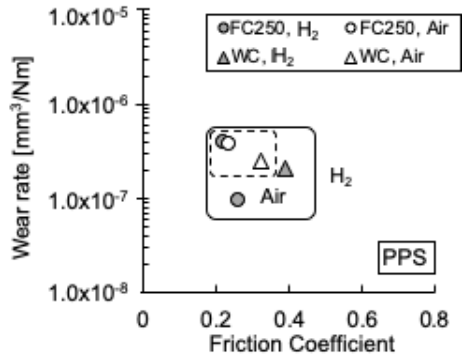

(d) PPS-filled PTFE

Fig.9 Comparison of friction and war of PTFE composite between hydrogen gas environment and ambient air

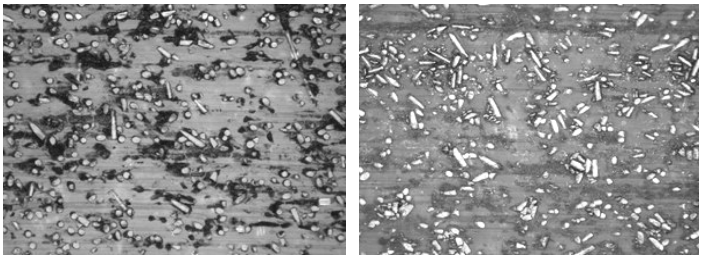

(a) GF, FC250, H_2 (b) GF, FC250, Air

Fig.10 Worn surface image of GF-filled PTFE

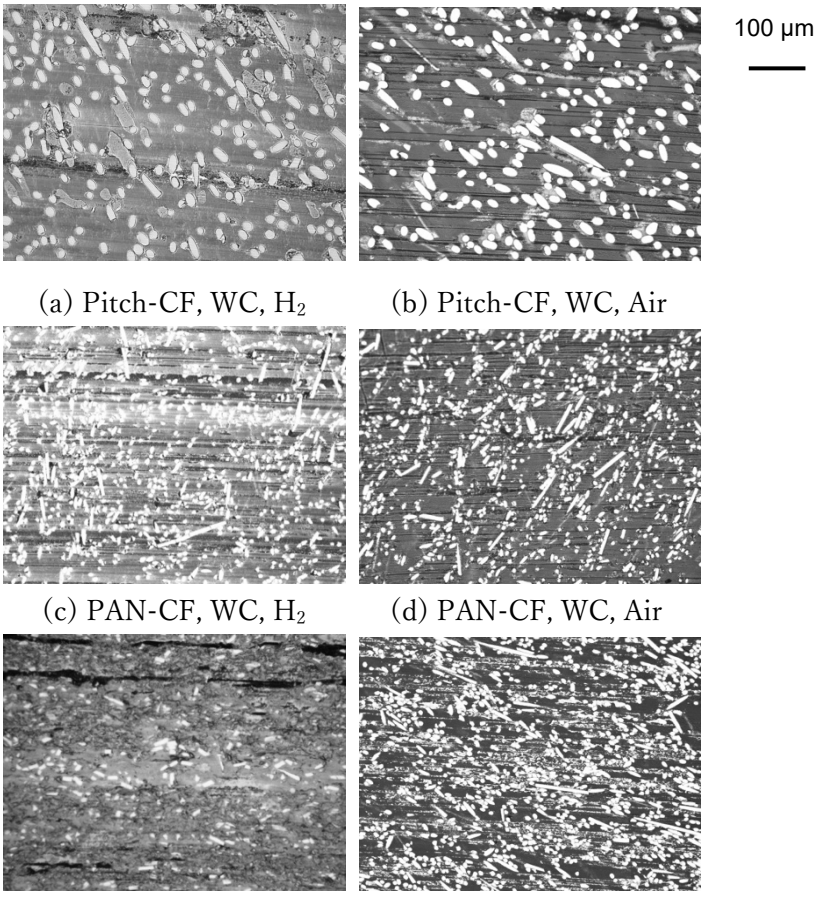

(a) Pitch-CF, WC, H_2 (b) Pitch-CF, WC, Air

(c) PAN-CF, WC, H_2 (d) PAN-CF, WC, Air

(e) PAN-CF, FC250, H_2 (f) PAN-CF, FC250, Air

Fig.11 Worn surface image of CF-filled PTFE composites

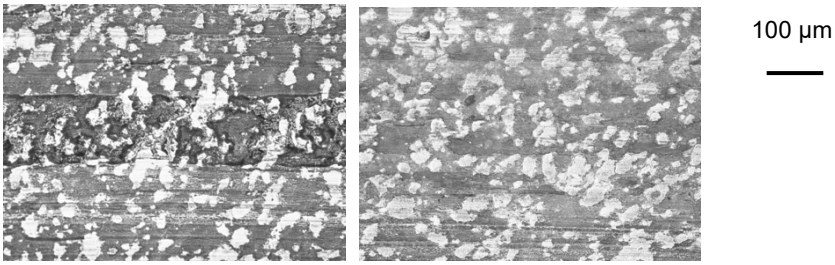

(a) PPS, WC, H_2 (b) PPS, WC, Air

Fig.12 Worn surface image of PPS-filled PTFE

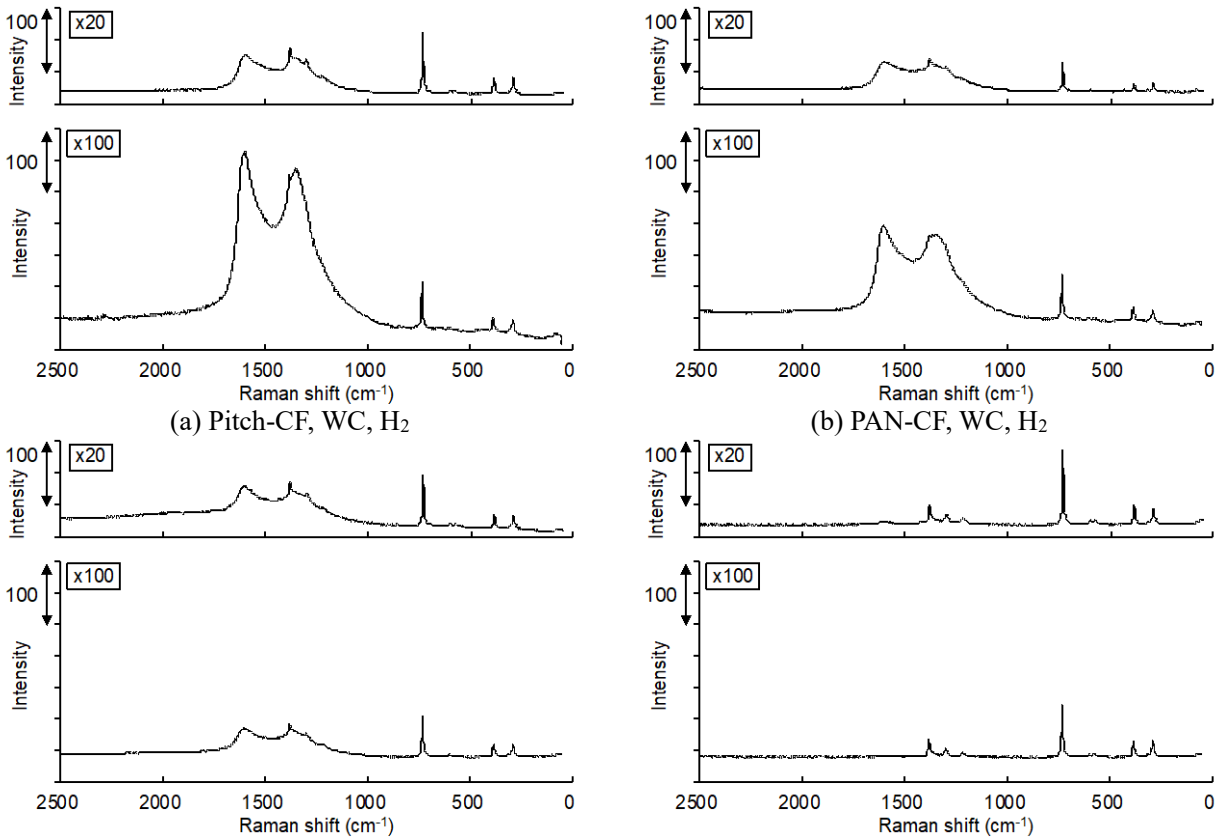

(a) Pitch-CF, WC, H_2 (b) PAN-CF, WC, H_2

(c) PAN-CF, FC250, H_2 (d) PAN-CF, FC250, Air

Fig.13 Representative Raman spectrum obtained from worn surface of CF-filled PTFEs

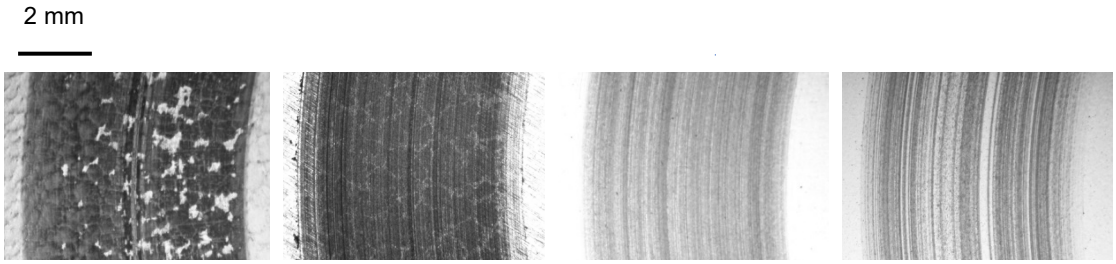

(a) FC250, H_2 (b) FC250, Air (c)WC, H_2 (d) WC, Air

Fig.14 Sliding track formed by GF-filled PTFE

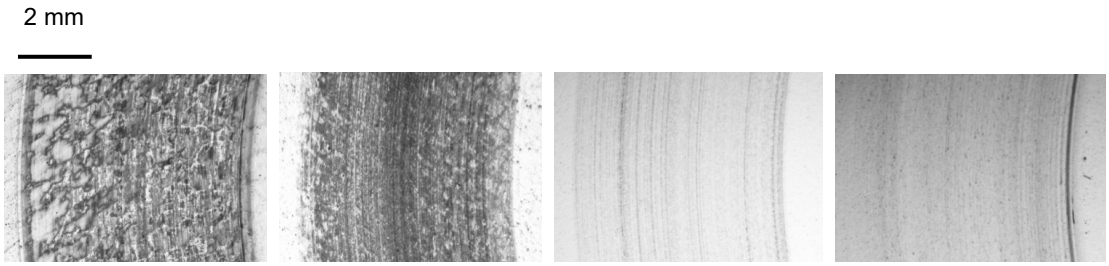

(a) FC250, H_2 (b) FC250, Air (c)WC, H_2 (d) WC, Air

Fig.15 Sliding track formed by Pitch-CF-filled PTFE

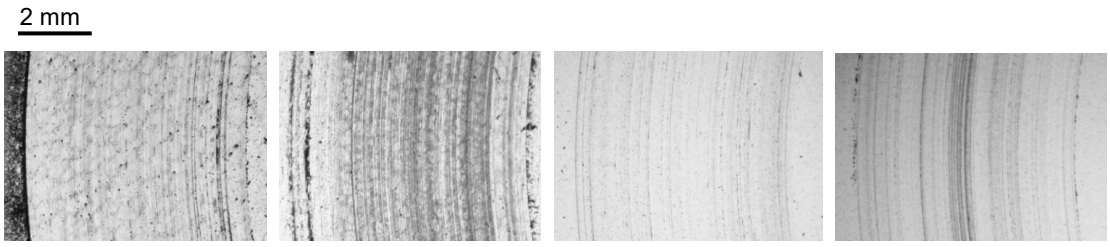

(a) FC250, H_2 (b) FC250, Air (c)WC, H_2 (d) WC, Air

Fig.16 Sliding track formed by PPS-filled PTFE

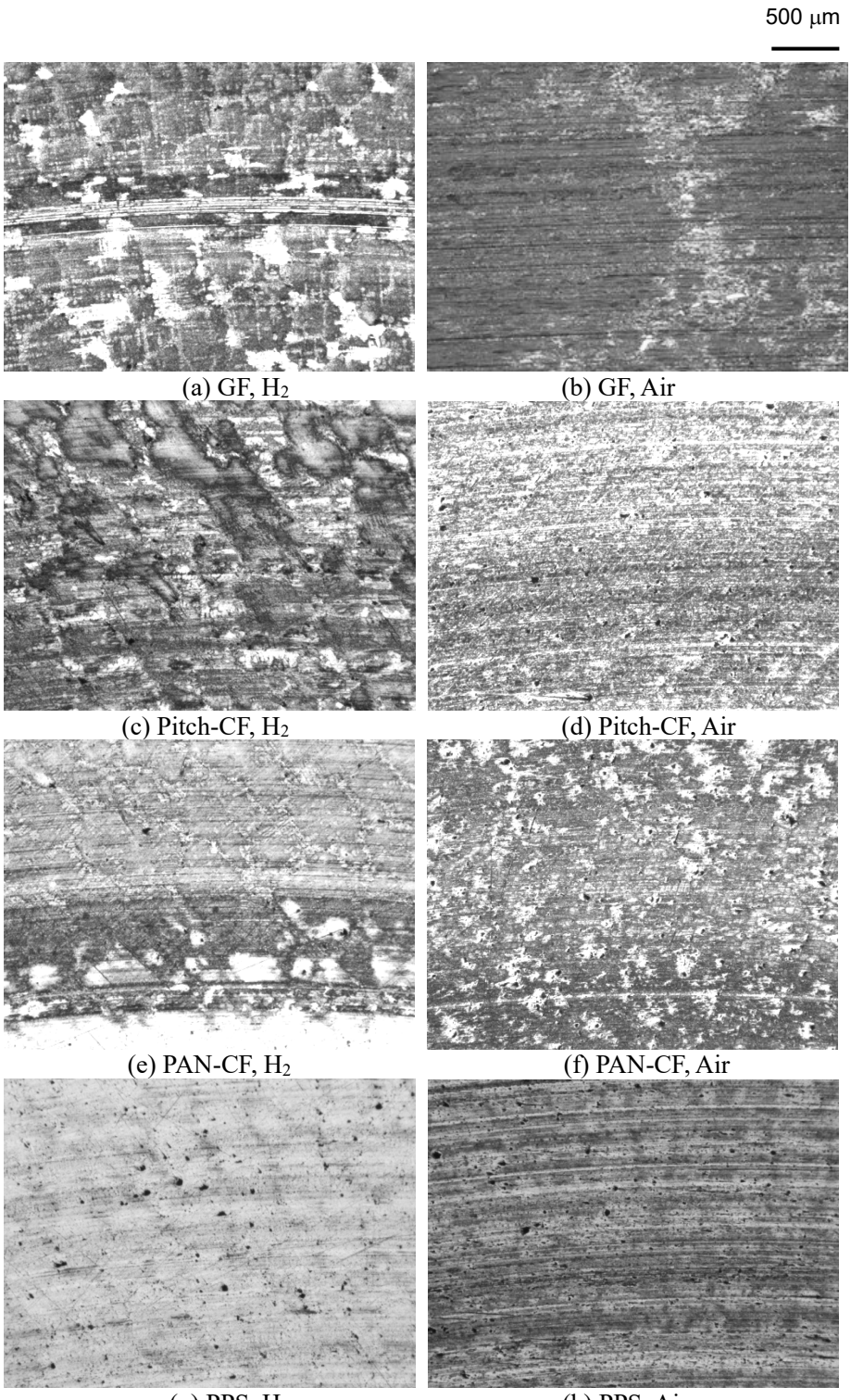

(a) GF, H_2 (b) GF, Air

(c) Pitch-CF, H_2 (d) Pitch-CF, Air

(e) PAN-CF, H_2 (f) PAN-CF, Air

(g) PPS, H_2 (h) PPS, Air

Fig.17 Microscopic image of sliding track formed on FC250 disk surface

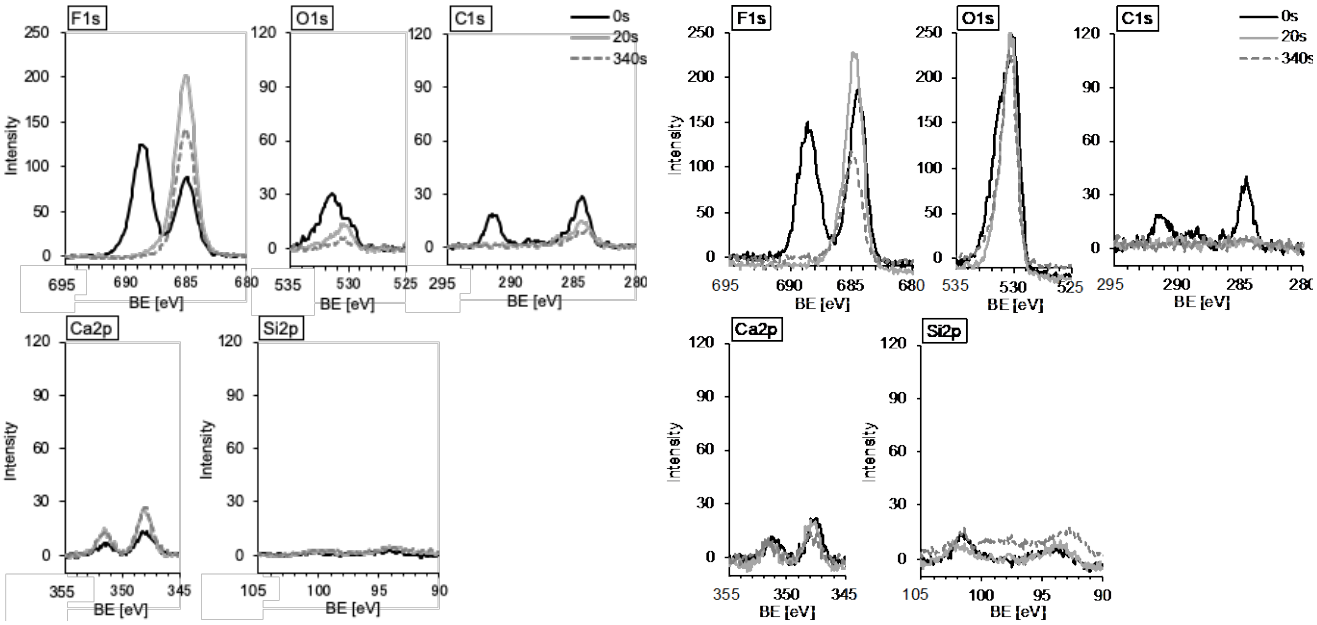

(a) GF, FC250, H_2 (b) GF, FC250, Air

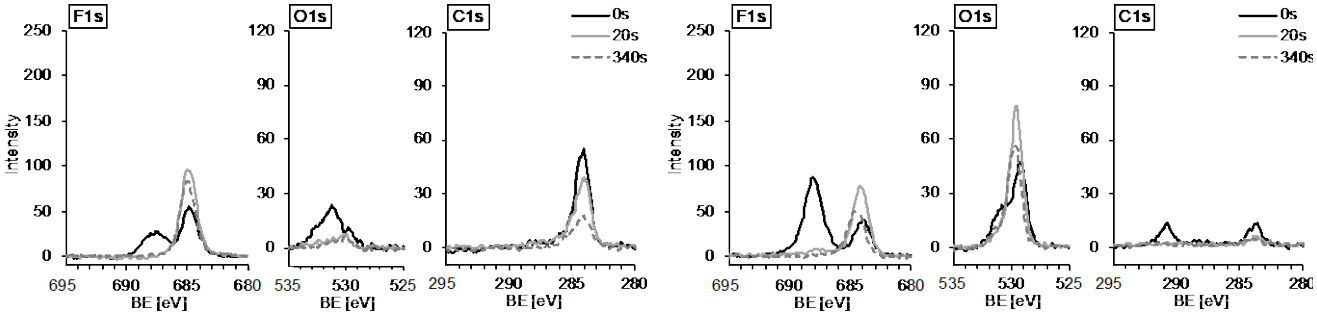

(c) Pitch-CF, FC250, H_2 (d) Pitch-CF, FC250, Air

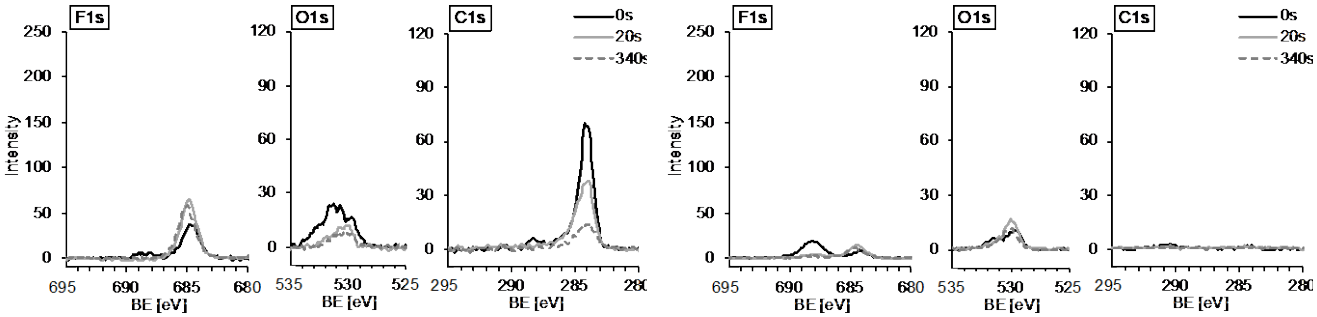

(e) PAN-CF, FC250, H_2 (f) PAN-CF, FC250, Air

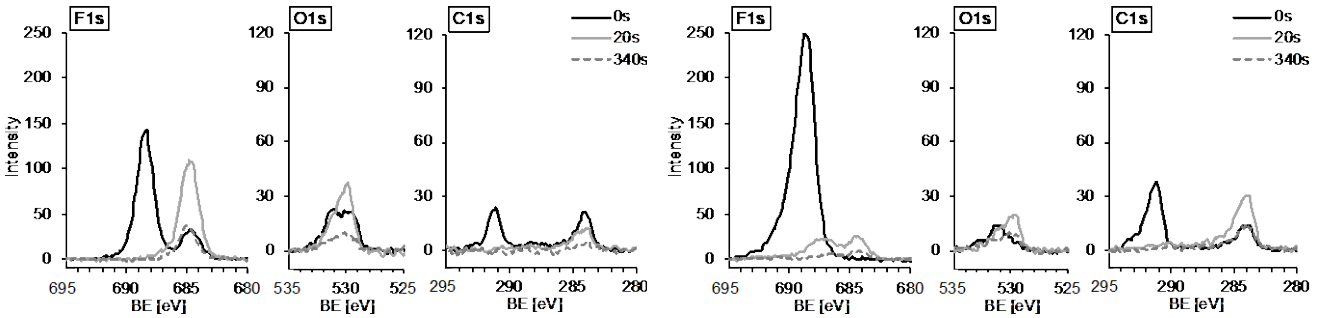

(g) PPS, FC250, H_2 (h) PPS, FC250, Air

Fig.18 XPS spectra obtained from sliding tracks formed on FC250 disk surface

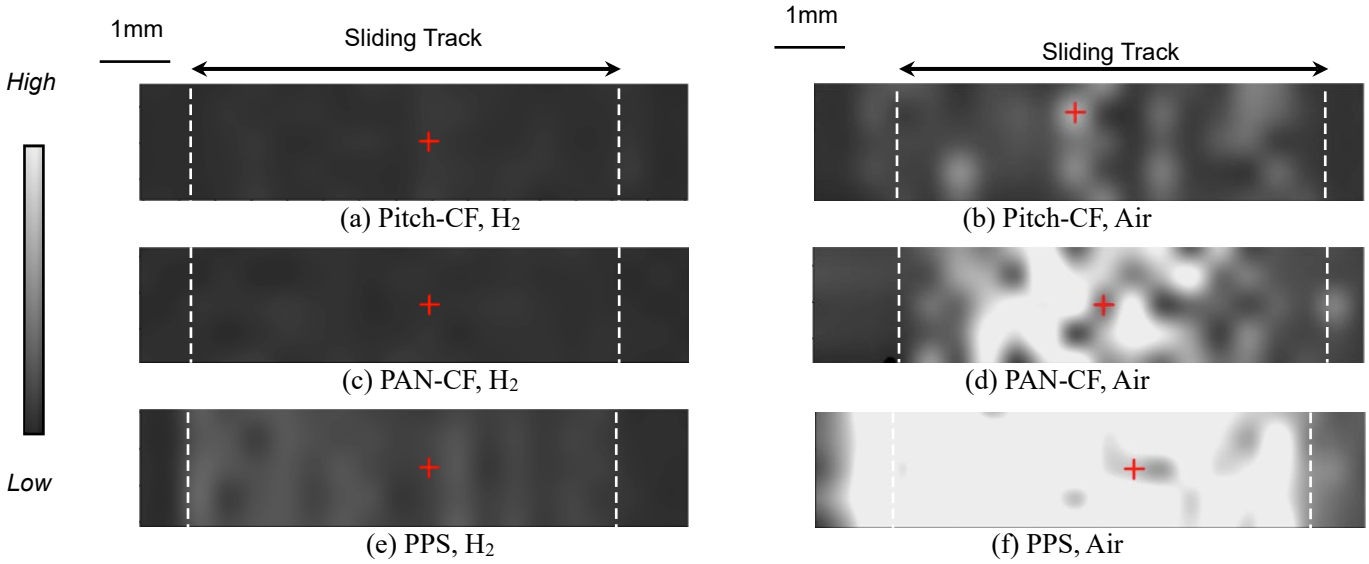

Fig.19 ATR mapping image of PTFE adhered on FC250 disk

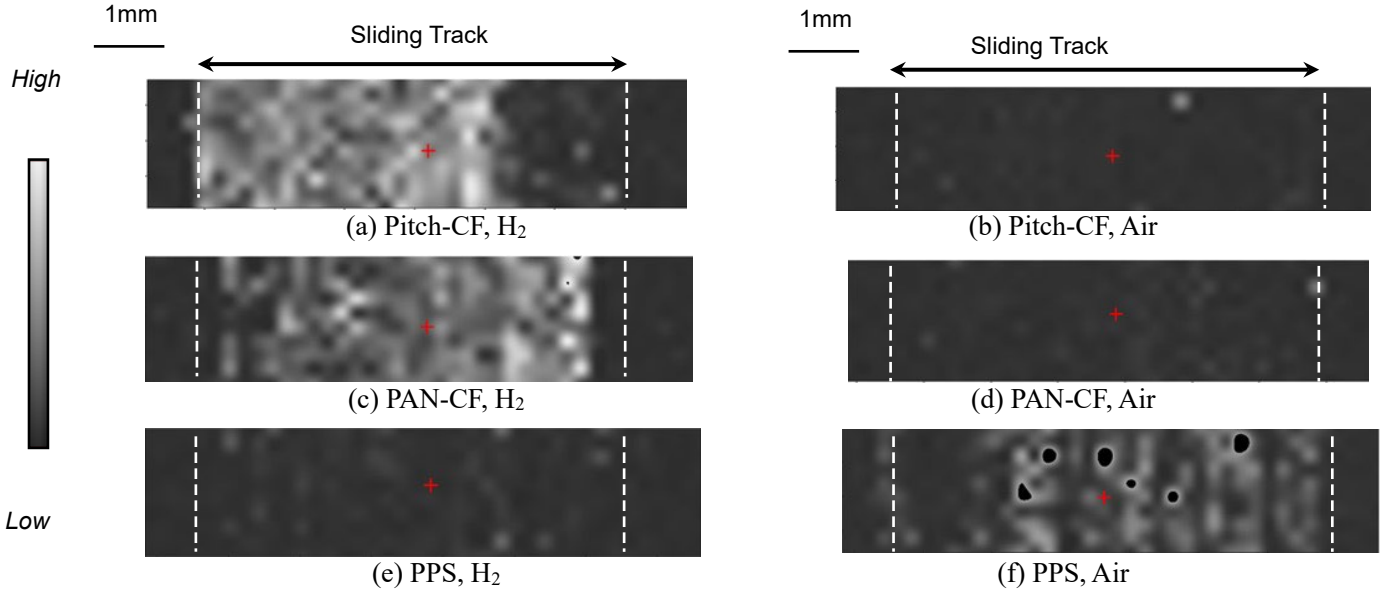

Fig.20 Raman mapping image carbon adhered on FC250 disk